This is a peer-reviewed, accepted author manuscript of the following article: Luo, X., Li, Z., Chang, W., & Cai, Y. (Accepted/In press). Laser-assisted grinding of reaction-bonded SiC. *Journal of Micromanufacturing*.

Laser-assisted grinding of reaction-bonded SiC

Abstract

The paper presents development of a novel laser-assisted grinding process to reduce surface roughness and subsurface damage in grinding reaction-bonded (RB)-SiC. A thermal control approach is proposed to facilitate the process development, in which a two-temperature model is applied to control the required laser power to thermal softening of RB-SiC prior to grinding operation without melting the workpiece or leaving undesirable microstructural alteration, while Fourier's law is adopted to obtain the thermal gradient for verification. An experimental comparison of conventional grinding and laser-assisted grinding shows significant reduction of machined surface roughness (37%-40%) and depth of subsurface damage (SSD) layer (22%-50.6%) using the thermal control approach under the same grinding conditions. It also shows high specific grinding energy 1.5 times that in conventional grinding at the same depth of cut which accounts for the reduction of subsurface damage as it provides enough energy to promote ductile-regime material removal.

Grinding, silicon carbide, laser-assisted, thermal control, subsurface damage

1. Introduction

Due to its superb properties such as chemical inertness, high carrier saturation velocity, high temperature-resistance, high specific stiffness, SiC is regarded as a promising material to replace silicon for the next generation of power electronics, quantum computing and semiconductor devices. However, it is one of the most hard-to-machine materials due to the high hardness and brittleness. Ductile-regime diamond grinding is an important manufacturing technique in the process chain for SiC, which usually delivers sub-micron level ground surface roughness with depth of subsurface damage of several microns. Time-consuming polishing therefore, has to be employed to further improve surface roughness down to nanometre level and remove subsurface damage layer. As a result, production cost of a SiC wafer is several times higher than a Si wafer of the same size. This has hindered the further development of SiC technology and its commercialisation.

In recent years ultrasonic assisted grinding has been developed to improve surface roughness in grinding brittle materials. Research shows that with ultrasonic frequency vibration of the grinding wheel, the critical depth of cut can be increased which enhances the ductile regime grinding condition and results in the reduced surface roughness [1]. As mechanical stress of materials normally decreases with increase of temperature due to thermal softening [2], laser-assisted grinding (LAG) has also been attempted to machine brittle materials in which 30% reduction in surface roughness was achieved compared with conventional grinding [3]. Very recently, a novel laser-assisted grinding process which used lasers for micro structuring Si_3N_4 ceramics improved material removal rate while slightly improving ground surface quality [4]. Wang et al. [5] revealed that the machined surface quality in LAM of Al_2O_3p/Al is improved and the tool wear can be reduced by 20-30% compared with conventional cutting. On the other hand, in the LAM of Al_2O_3 ceramics, Chang and Kuo [6] found the feed and thrust cutting forces can be reduced by 22% and 20%, respectively. Also, Guerrini et al. [7] induced thermal cracks by laser radiation before grinding sintered reaction Si_3N_4, which showed the average force decreased by 26%-27% once again. While, the researcher not only focus on the machining force, the material removal mechanism of LAM was another key research. The surface of silicon nitride workpiece was oxidized and formed an amorphous silicate, which could reduce the hardness, and finally promoting the material removal rate and benefit to the tool wear [8]. However, these researches mostly focused on reduction of machined surface roughness, forces and removal mechanism. The study on new process control to minimize subsurface damage is rare. In fact, level of subsurface damage is a significant surface quality characterisation parameter as it influences performance of the final products. In laser-assisted grinding, control of the pre-heat level is crucial to success.

In this study, a thermal control approach is proposed to facilitate development of a novel laser-assisted grinding process for RB-SiC. An experimental study is carried out to evaluate the effectiveness of this approach in comparison with conventional grinding in relation to surface roughness and depth of subsurface damage layer of the ground RB-SiC. The mechanism of laser pre-heat on the reduction of sub-surface damage is investigated from the point of view of specific grinding energy.

2. Thermal control in laser-assisted grinding

In laser-assisted grinding the material removal temperature T_s, which is defined as the average temperature of the material as it enters the grinding zone, plays an important role. It has to be controlled precisely to achieve the full benefits of laser-assisted grinding without melting the workpiece or leaving undesirable microstructural alteration in the machined workpiece.

During laser preheating, the laser thermal energy is firstly absorbed by the electrons in the SiC. After that, the thermal energy is transferred from the electrons to the lattices of the SiC by thermal conduction although some energy is lost due to thermal diffusion. Laser energy density and laser power are two critical laser machining parameters to be controlled in laser-assisted grinding. The study adopts a two-temperature model (TTM) to obtain them. In this model, the electrons and lattices are treated as two separate heat baths with temperature T_e and T_l respectively. The diffusion equation between the electrons and the lattices can be described as [9]:

$$C_e \frac{\partial T_e}{\partial t} = -\frac{\partial Q(z)}{\partial z} - \gamma(T_e - T_l) + S \quad (1)$$

$$C_l \frac{\partial T_l}{\partial t} = \gamma(T_e - T_l) \quad (2)$$

Where C_e, C_l, and z are the heat capacities of the electron and the lattice, and the ablation rate to SiC, respectively. $Q(z)$ is the electron heat flux and it can be calculated as: $Q(z)$=-ke∂Te/∂z. k_e is the electron thermal conductivity. S is the absorbed energy. The electrons and lattices are in thermal equilibrium state, i.e. $T_e = T_l$. Therefore, equation (1) can be simplified as:

$$C_e \frac{\partial T_e}{\partial t} + \frac{-ke\,\partial Te/\partial z}{\partial z} = S \quad (3)$$

The absorbed energy S in equation (3) can be expressed as:

$$S = I(t)A_b\alpha e^{-\alpha z} \quad (4)$$

Where $I(t)$ is the laser intensity. A_b and α are the surface transmissivity and optical penetration depth of RB-SiC, respectively. The temperature of the electrons can be described by integration of equation (1):

$$T_e = \left[\frac{2I(t)At\alpha e^{-\alpha z}}{\dot{C_e}}\right]^{\frac{1}{2}} \quad (5)$$

The temperature of the lattice can be simplified as $T_l \approx T_e t/C_l$. As it can also be determined by the average cooling time of the electrons ($t = \dot{C_e} T_e/2$), so it will have

$$T_l \approx T_e^2 \frac{\dot{C_e}}{2C_l} \approx \frac{F\alpha}{C_l} e^{-\alpha z} \quad (6)$$

Where F is the laser energy density. The ablation threshold, $F_0 \approx T_l C_l/\alpha$ can be described by the Arrhenius-type equation. Equation (6) can be written as:

$$F \approx F_0 e^{\alpha z} \quad (7)$$

The ablation threshold and the optical penetration depth for SiC are 1.5 J/cm^2 and 1.7 μm^{-1}, respectively. The ablation rate is 1.8 um/pulse. Therefore, the energy density can be obtained through Eq. (7) as 0.07 J/cm^2.

According to the definition of the energy density, the power of the laser system (P) to be used in the laser deburring process can be obtained as:

$$P = F F_r A \quad (8)$$

Where F_r and A are the laser frequency and area of the laser spot respectively.

A laser wavelength of 1064nm is used with a laser spot of 4 mm diameter. The calculated maximum laser power below the laser ablation threshold is 88 W.

As laser preheating will always result in non-steady-state heat conduction, the surface temperature heated by the laser can be calculated by Fourier's law, which can be described as:

$$\nabla^2 T = \frac{\rho c}{k}\frac{\partial T}{\partial t} - \frac{A_v I(x,y,z,t)}{k} \quad (9)$$

where T is the temperature of the workpiece, ρ and c are the density and the specific heat of the workpiece, respectively. k is the thermal diffusivity of the workpiece. A_v is the fraction of the radiation energy absorbed per unit volume of the workpiece and I is the Gaussian distribution of the intensity.

It is assumed that in a laser-assisted grinding process, radiation and convection are not significant sources of heat loss and are therefore negligible. The complete solution for the uniform, constant irradiance is:

$$T(z_c,t) = \frac{2I_0}{k}\left[\left(\frac{\kappa t}{\pi}\right)^{\frac{1}{2}} e^{(-z_c^2/4kt)} - \frac{z_c}{2} erfc\frac{z_c}{\sqrt{4\kappa t}}\right] \quad (10)$$

Where

$$\kappa = \frac{k}{\rho c} \quad (11)$$

$$erf(s) = \frac{2}{\sqrt{\pi}}\int_0^s e^{-x^2} dx \quad (12)$$

Where *erf(s)* is the error function and *erfc(s)* is the complementary error function equal to *1-erf(s)*. I_0 is the irradiance and z_c is the depth coordinate radiated into the sample. The surface temperature of the semi-infinite solid is given by:

$$T_s(0,t) = \frac{I_0}{k}\left(\frac{4\kappa t}{\pi}\right)^{1/2} \quad (13)$$

Eq. (13) shows that temperature rise is caused by releasing the heat (F_q) per unit area. Note that for very long heating durations ($t \to \infty$), the temperature increases on the surface, $T \sim \sqrt{t}$ would be unlimited. This is useful for estimating the time required to reach a specified surface temperature for a given laser irradiation. The material properties of RB-SiC shown in Table 1 have been used in the calculations.

Table 1
Material property of RB-SiC in this study

Items	RB-SiC
Elastic modulus (GPa)	390
Vickers hardness (Kgf·mm^{-2})	3000
Compressive strength (MPa)	2000
Fracture toughness K_{IC} (MPa·m$^{1/2}$)	4.0
Thermal Expansion Coeff. ×10^{-6}/^{o}C	3
Thermal conductivity (W/mK)	150
Thermal Shock Resistance ^{o}C	400
Melting point (K)	3000
Specific heat Capacity (J/kgK)	1100
Density ρ (g/cm^3)	3.1

Note: the parameters listed in Table 1 are supplied by Goodfellow Cambridge Ltd.

According to Eq. (10) and (13) the surface temperature can be obtained. Fig.1 shows the theoretical thermal gradient through the thickness of a workpiece 60 s after laser heating (at a laser power of 80 W). It can be seen that the maximum surface temperature of 2,060K is achieved while the lowest temperature of 1210 K appears at a depth 10 μm below the surface which helps to harvest the benefit of high surface temperature without changing the integrity of the workpiece.

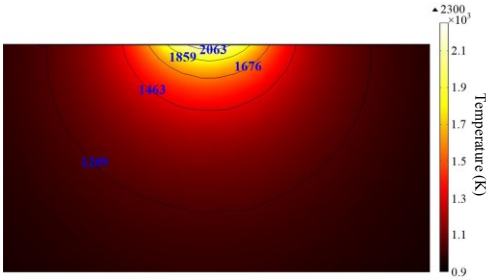

Fig. 1. Thermal gradient of RB-SiC under a laser power of 80 W, wavelength of 1064 nm, spot size of 4 mm diameter

3. Experimental setup and machining conditions

To evaluate the effectiveness of laser-assisted grinding surface grinding trials were carried out on a 6-axis ultra-precision hybrid machine developed at the University of Strathclyde. The machine was equipped with four high precision linear air bearing slides (full stroke motion accuracy was better than 0.1μm) and two rotational axes (motion accuracy better than 20 and 10 arcsec, respectively). Experimental set up on this machine is shown in Fig. 2. The left vertical *Z* axis carries a high-speed spindle (max spindle speed 60,000 rpm with runout less than 1μm) for grinding while the other vertical *W* axis carried a fibre laser head for preheating. The laser (IPG, YLR-200-MM-AC-11) had a wavelength of 1064 nm. A focusing lens was mounted on the *W* axis and connected to the laser via an optical fibre, allowing arbitrary motion between the laser spot and the workpiece. The intense laser radiation was projected peripheral to the grinding area on the RB-SiC surface in front of the engaging grinding wheel by a reflection mirror. The projected laser spot had a diameter of 4 mm.

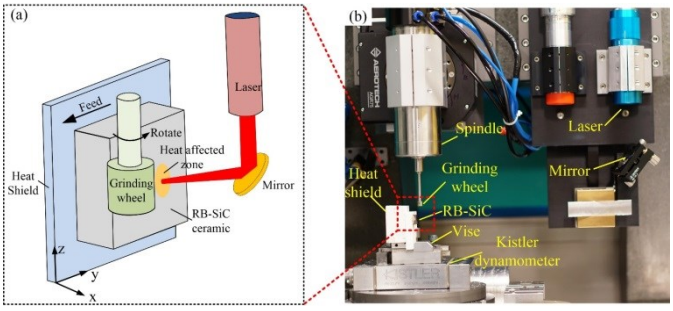

Fig. 2 Laser-assisted grinding experimental setup (a) Schematic diagram of the setup and (b) Hardware setup.

The RB-SiC specimen with a dimension of 12.5 mm×12.5 mm×5 mm (length, width and height) was fixed on a three-component

dynamometer (Kistler 9129) through a vice. A heat shield was used to insulate the heat to protect the vice and dynamometer. Resin bond diamond grinding wheels with a wheel diameter of 6 mm, a grit size of 15 μm and 100% concentration were trued and dressed to a run-out less than 1 μm for use in the surface grinding trials.

In the laser-assisted machining trial laser powers of 20 W, 40 W, 80 W and 100 W were used to preheat the RB-SiC specimen for 60 s with a scanning speed of 12.5 mm/min. To fully assess the capability of the laser-assisted grinding process conventional grinding trials have also been performed under the same machining conditions, i.e. with a spindle speed of 8000 rpm, a feed rate of 2 mm/min at a depth of cut of 5 μm, 10 μm, 15 μm and 20 μm, respectively.

The grinding forces were measured by the dynamometer during the grinding trials. An infrared thermometer (IR-750-EUR BEHA-AMPROBE, working range of 50°C–1550°C, accuracy of ±1.8% and response time of 0.25s) was used to measure the in-line temperature of the RB-SiC surface.

The machined surface topography was inspected by a scanning electron microscope (SEM) (FEI Helios Nanolab 600i). The machined surface roughness Ra was measured by a white light interferometer (Zygo CMP-200) at five different locations, with an average value as the final result. To measure the depth of subsurface damage, ion cross-section polishing was used (IB-09020CP ion polisher). To reduce random errors, four different positions were measured for each RB-SiC specimen.

4. Results and discussions

4.1. Surface topography

Fig. 3 shows surface topography of the ground surface in both conventional grinding and laser-assisted grinding. Brittle fractures were very evident on surface ground by conventional grinding, while the density of brittle fracture was reduced with decrease of depth of cut. The density of brittle fracture was dramatically reduced on ground surfaces obtained by laser-assisted grinding. As calculated in section 2, 80 W is very close to the required laser power. The measured surface temperature near the grinding spot is 1980K which is very close to the calculated value shown in Fig.1. At high temperature, material removal is predominantly in the ductile regime, while at the laser power of 100 W, the density of brittle fracture on the ground surface has increased although it is still less than 5%.

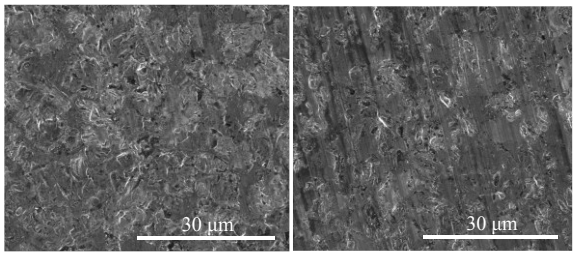

(a) Depth of cut 10μm (b) Depth of cut 5μm

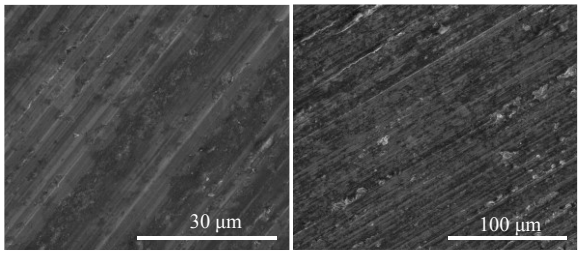

(c) Laser power 80 W (d) Laser power 100 W (both at Depth of cut 10μm)

Fig. 3 Surface topography of ground surfaces in both conventional grinding and laser-assisted grinding (spindle speed 8,000 rpm, feed rate 2 mm/min)

The reduction of the machined surface roughness Ra by laser-assisted grinding is further confirmed in Fig. 4 in which an improvement of 37%-40% was observed under the laser power of 80 W when depth of cut varies from 5 um to 20 μm. However, at the laser power of 20 W there is almost no change in surface roughness Ra which indicates that the greater laser preheating was now powerful enough to soften the material. A slight reduction of surface roughness was seen at the laser power of 40 W as laser heat started to soften material. Fig. 4 also shows that although 22% to 30% improvement was achieved at the laser power of 100 W, the machined surface roughness was worse than at 80 W due to overheating. This observation was demonstrated by Vickers hardness tests. The tests showed that hardness started to drop only when the laser power was larger than 30 W. When the laser power reached 70 W, the hardness of RB-SiC was dramatically decreased to 2480 HV from the original 2920 HV at the laser power of 20 W [10].

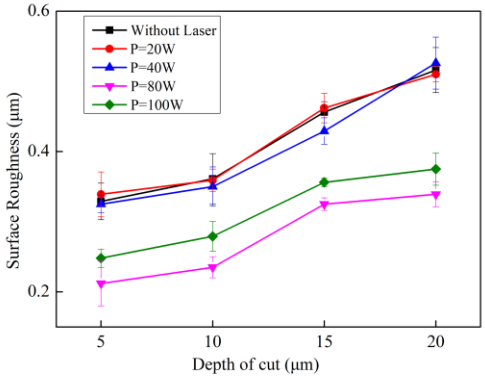

Fig. 4. Comparison of attainable surface roughness Ra of the ground RB-SiC by conventional grinding and laser-assisted grinding.

4.2. Subsurface damage

Grinding induced subsurface damage of brittle materials has been extensively studied in the past [11, 12]. Materials properties of work materials (fracture toughness and hardness), wheel geometry and type (grit size, geometry, bond materials etc.), dynamic stiffness of the grinding machine and grinding parameters can all influence the level of subsurface damage [13, 14]. Fig. 5 shows the comparison of subsurface damage of ground RB-SiC by conventional grinding and laser-assisted grinding at the laser power of 80 W. Very small microcracks were observed underneath the ground surface in a layer with depth of 1.84 μm in conventional grinding with the depth of cut of 5 μm. The depth of damage was limited by the compliance provided by the resin bond grinding wheel. However, as depth of cut increased, a big lateral crack appeared at 8.6 μm underneath the ground surface. When using laser-assisted grinding only small micro-cracks were observed and significant reduction of depth of subsurface damage (22% to 50.6%) was achieved.

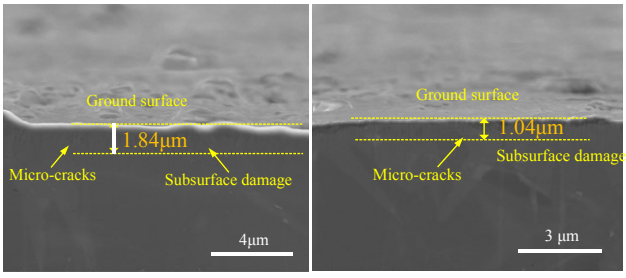

(a) Conventional grinding (b) LAG (Laser power, 80W)
(Spindle speed 8000rpm，feed rate 2 mm/min, depth of cut 5μm)

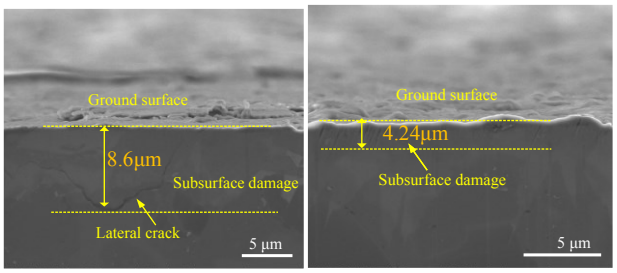

(c) Conventional grinding (d) LAB (laser power, 80W)
(Spindle speed 8000rpm, feed rate 2mm/min, depth of cut 20μm)

Fig. 5 Comparison of subsurface damage in conventional grinding and laser-assisted grinding (LAG).

4.3. Specific energy

To further explain the effect of laser heating on subsurface damage on the ground RB-SiC, specific grinding energy e_c in the machining trial was calculated. Specific grinding energy can be described as:

$$E = \frac{F_t V_s}{a V_w b} \quad (14)$$

Where F_t, v_s, a_p, v_w *and* b are tangential grinding force, wheel speed, depth of cut, work speed and cutting width, respectively. The material removal mechanism in grinding RB-SiC is complex. It involves both brittle fracture and plastic deformation. However, ductile-regime material removal requires higher specific energy than brittle fracture [15] as it requires more energy to initiate dislocations. Fig. 6 (a) illustrates the variation of specific grinding energy in the machining trials. In conventional grinding when the depth of cut increased from 5 μm to 20 um the specific energy decreased from 465 J/mm³ to 318 J/mm³. It indicates that the material removal regime changed from predominantly ductile to predominantly brittle as reflected in the ground surface topography shown in Fig. 3. At 5 μm depth of cut, the specific grinding energy in LAG process was increased to 712 J/mm³ at the laser power of 80 W. The measured tangential grinding force and normal grinding force in comparison with conventional grinding is shown in Fig. 6 (b). It can be seen that the tangential force in LAG process becomes profound (53% of the overall grinding force) and it is larger than in conventional grinding (20% of the overall grinding force). It explains why specific grinding energy in LAG process is larger than conventional grinding. The results show that laser-preheating increases specific grinding energy. This is consistent with increasing the proportion of ductile removal. As a result, subsurface damage can be reduced.

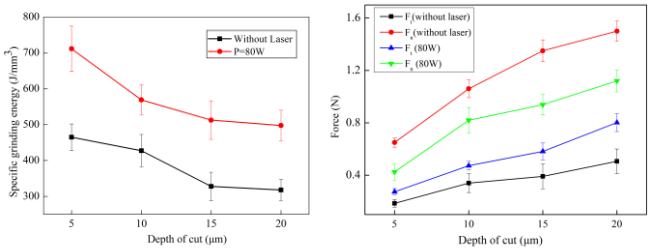

(a) Specific grinding energy (b) Grinding force

Fig.6 Specific energy and grinding force in conventional in conventional grinding and LAG of different laser power at different depth of cuts.

5. Conclusion

The paper presents results for the development of laser-assisted grinding for RB-SiC. The following conclusions can be drawn:

- Combining the two-temperature model and Fourier's law, the laser power for laser heating can be calculated and used to control the surface temperature and thermal gradient in order to benefit from high surface temperature in terms of reduction of hardness in a thin layer of work material without changing the integrity of the workpiece after grinding.
- Laser-assisted grinding can significantly reduce the surface roughness and subsurface damage.
- Increase of specific energy in LAG process can enhance the ductile-regime condition and result in low subsurface damage in ground RB-SiC.

Date statement:

All data underpinning this publication will be available from the University of Strathclyde Knowledge Base.

Acknowledgement

The authors would like to thanks the UK EPSRC (EP/K018345/1), China's NKR&D Programs (2016YFB1102204) & 973 (2011CB013202) for the financial supports of this study.

References

[1] Liang, Z., Wang, X., Wu, Y., Xie, L., Jiao, L., Zhao, W., 2013, Experimental study on brittle-ductile transition in elliptical ultrasonic assisted grinding (EUAG) of monocrystal sapphire using single diamond abrasive gran, International Journal of Machine Tools & Manufacture, 71: 41-51.

[2] Melkote, S., Kumar, M., Hashimoto, F., Lahoti, G., 2009, Laser-assisted micro milling of hard-to-machine materials, Annals of the CIRP, 41/1: 45-48.

[3] Chang, W., Luo, X., Zhao, Q., Sun, J. Zhao, Y., 2012, Laser assisted micro grinding of high strength materials, Key Engineering Materials, 496: 44-49.

[4] Azarhoushang, B., Soltani, B., Daneshi, A., 2018, Study of the effects of laser micro structuring on grinding of silicon nitride ceramics, Annals of the CIRP, 67/1: 329-332.

[5] Wang, Y.,Yang, L.J., . Wang N.J.,2002, An investigation of laser-assisted machining of Al2O3 particle reinforced aluminum matrix composite, J. Mater. Process. Technol. 129, 268–272.

[6] Chang, C., Kuo, C., 2007, An investigation of laser-assisted machining of Al2O3 ceramics planing, Int. J. Mach. Tools Manuf. 47, 452–461.

[7] Guerrini, G., Lutey, A.H.A., Melkote, S.N., Fortunato, A., 2018, High throughput hybrid laser assisted machining of sintered reaction bonded silicon nitride, J. Mater. Process. Tech. 252 , 628–635.

[8] Lee, S., Kim, J., Suh, J.,2014, Microstructural Variations and Machining Characteristics of Silicon Nitride Ceramics from Increasing the Temperature in Laser Assisted Machining, Int. J. Precis. Eng. Manuf. 15, 1269–1274.

[9] Wellershoff, S.-S, Hohlfeld, J., Gudde, J., atthias, E., 1999, The role of electron-phonon coupling in femtosecond laser damage of metals, Appl. Phys. A: Mater. Sci. Process. 69S: 99-107.

[10] Li, Z, Zhang, F., Luo, X., Chang, W., Cai, Y., Zhong, W., Ding, F., Material removal mechanism of laser-assisted grinding of RB-SiC ceramics and process optimisation, Journal of the European Ceramic Society (in press).

[11] Inasaki., I, 1987, Grinding of hard and brittle materials, Annals of the CIRP, 36/2: 463-471.

[12] Brinksmeier, Mutlugunes, Y., Klocke, F., Aurich, J. C., Shore, P., Ohmori, H., 2010, Ultra-precision grinding, Annals of the CIRP, 59/2: 652-671.

[13] Zhang, B., Howes, T. D., 1995, Subsurface evaluation of ground ceramics, Annals of the CIRP, 44/1: 263-266.

[14] Schnurbusch, G., Brinksmeier, E., Riemer, O., 2017, Influence of cutting speed on subsurface damage morphology and distribution in ground fused silica, Inventions, 2(3), 15.

[15] Bifano, T. G., Fawcett, S. C., 1991, Specific energy as an in-process control variable for ductile-regime grinding, Precision Engineering, 256-262.